Preprints of the 21st IFAC World Congress (Virtual)
Berlin, Germany, July 12-17, 2020

Sum of squares approach for ground vehicle lateral control under tire saturation forces ⋆

Alexandre M. Ribeiro * **André R. Fioravanti** *
Alexandra Moutinho ** **Ely C. de Paiva** *

* *School of Mechanical Engineering, Mendeleyev Street 200, 13083-860, Campinas, Brazil (e-mails: {amribeiro, fioravanti, elypaiva}@fem.unicamp.br).*
** *IDMEC, LAETA, Instituto Superior Técnico, Universidade de Lisboa, Av. Rovisco Pais, 1049-001 Lisbon, Portugal (e-mail: alexandra.moutinho@tecnico.ulisboa.pt)*

Abstract:
This work presents the stability analysis and design of a lateral controller for a nonlinear ground vehicle applying the concept of polynomial sum of squares relaxations. The system is approximated by a polynomial vector field that describes the lateral vehicle dynamics. The resulting polynomial system falls on a class of non-affine in input system, which makes the control synthesis more involved. This issue is circumvented by an input-affine approximation, simplifying the stability analysis and the design procedure of a polynomial state-feedback controller able to enlarge the region of attraction (RoA). We also compare the estimated region of attraction with the standard LQR optimal controller.

Keywords: Vehicle stability, sum of squares programming, region of attraction, nonlinear controller synthesis, vehicle dynamics, input saturation.

1. INTRODUCTION

One of the fundamental concerns in systems and control theory is that of determining the stability of an equilibrium point of a dynamical system. Among existing methods, those based on Lyapunov functions are even nowadays dominant in literature (Summers (2013); Khodadadi et al. (2014); Nikravesh (2018); Ahmadi and Majumdar (2019)).

Recently, besides the advances on polynomial optimization based on sum of squares (SOS) relaxations, significant research has been performed on the development of Lyapunov-based analysis tools for computing regions of attraction (Tacchi et al. (2018)), reachability sets (Jones and Peet (2019)), reach-avoid sets (Landry et al. (2018)) and for nonlinear control synthesis (Singh et al. (2019)).

Regarding vehicle stability, estimating the region of attraction (RoA) is an important subject of study. The RoA is a safe subset of the state space in which the equilibrium point is stable, in other words, it describes the boundary on how far from equilibrium the vehicle can reach where stability is assured. Such characteristics respond if an unintentionally spin is still safe or will lead to divergence. Early works have mainly relied on linear systems theory to guarantee local stability. Lyapunov's second method was first used in Johnson and Huston (1984) with a linearized vehicle model. The RoA estimate was then found manually by calculating the largest level set of the candidate function that fits within the region. Since then, Lyapunov-based methods were used aiming more accurate and representative estimates of the RoA (Sadri and Wu (2012); Németh et al. (2016); Masouleh and Limebeer (2017)).

For general nonlinear systems, there is still no convex optimization method that can be used to search for a Lyapunov function. However, restricting our search to a class of polynomial vector field systems and considering the Lyapunov function strictly written as a sum of squares polynomial form, the problem can be tractable by convex optimization (Parrilo (2003)).

The main contributions of this paper are threefold: first, we extend the sum of squares algorithm proposed in Jarvis-Wloszek et al. (2005) and Masouleh and Limebeer (2017) to address the control problem for the class of non-input-affine systems; second, the control design synthesis is evaluated under input saturation with a detailed discussion about numerical issues and computational complexity; and third, we evaluate the SOS approach on a realistic nonlinear model of a ground vehicle which is a challenging system due to the tire-ground interaction dynamics.

The remainder of the paper is organized as follows. In Section 2 we provide the necessary background about the SOS theory. Section 3 shows the vehicle mathematical

⋆ This work was supported by FCT, through IDMEC, under LAETA, project UIDB/50022/2020. The mobility of A. Ribeiro has been possible with the Erasmus Mundus SMART^2 support (Project Reference: 552042-EM-1-2014-1-FR-ERA MUNDUS-EMA2) coordinated by CENTRALESUPELEC. The authors also acknowledge the support of FAPESP through Regular project AutoVERDE N. 2018/04905-1, Ph.D. FAPESP 2018/05712-2, CNPq grant 305600/2017-6 and Project INCT-SAC - (CNPq 465755/2014-3, FAPESP 2014/50851-0).

model and the polynomial vector field approximation. In Section 4 we propose an affine transformation to use the tools provided by the SOS decompositions. Section 5 deals with estimations of the region of attraction under open- and closed-loop analysis. In Section 6 we compare the SOS technique with the traditional LQR controller. Finally, in Section 7 we give our conclusion and suggest ideas for future work.

2. BACKGROUND DEFINITIONS AND THEOREMS

2.1 SOS applied to system stability analysis

A polynomial $p(x)$ is SOS if it can be decomposed into the sum of the square of n polynomials, i.e., $p(x) = \sum_{i=1}^{n} p_i^2(x)$ where $p_i(x) \in \mathbb{R}[x]$. Here we denote by $\mathbb{R}[x]$ the set of real polynomials and by Σ_n the set of SOS polynomials in n variables.

We are concerned about the stability of equilibrium points characterized in the sense of Lyapunov. The systems of interest are described as a set of coupled ordinary differential equations of the form:

$$\dot{x} = f(x) + g(x)u, \tag{1}$$

where $x \in \mathbb{R}^n$ is the state variables, $u \in \mathbb{R}^m$ is the control input vector, $f : \mathcal{D} \to \mathbb{R}^n$ is a vector of polynomial state functions, $g : \mathcal{D} \to \mathbb{R}^{n\times m}$ is a matrix of polynomial control functions, with $\mathcal{D} \subset \mathbb{R}^n$. Without loss of generality, it is assumed that the equilibrium point of interest $\bar{x} \in \mathcal{D}$ is at the origin of $\mathbb{R}^n$.

In the robotic field, global asymptotic stability is hardly verified. Due to the nature of these systems, it is more likely to see a domain of attraction locally arranged around the equilibrium point.

The following result provides sufficient conditions for local asymptotic stability of (1) (Khalil (2002)):

Lemma 1. Let $u \equiv 0$. If there exists $\gamma > 0$ and a continuously differentiable function $V : \mathcal{D} \to \mathbb{R}$ such that

(1) $V(0) = 0$ and $V(x) > 0$ for all $x \in \mathcal{D}\backslash\{0\}$,
(2) $\Omega_\gamma = \{x \in \mathcal{D} \mid V(x) \leq \gamma\}$ is bounded,
(3) $\Omega_\gamma \subset \{x \in \mathcal{D} \mid \dot{V}(x) = \frac{\partial V}{\partial x} f(x) < 0\}\backslash\{0\}$,

then the open-loop solution of (1) asymptotically converges to the origin for any initial condition x_0 within Ω_γ. In this case, Ω_γ is called a domain of attraction of the trivial solution.

The problem of finding a Lyapunov function that satisfies the non negativity conditions can be converted into a convex problem using the SOS relaxation technique. In agreement with Lemma 1, we can estimate the region of attraction size by finding the largest level set γ of a Lyapunov function on which the stability conditions hold.

Additionally, the approach can be extended to a state feedback controller design intending to expand these regions. Allowing input u to be generated by a polynomial $K(x)$, Lemma 1 can be extended to the closed-loop system. Following Jarvis-Wloszek et al. (2005) and Papachristodoulou (2005), an SOS program able to tackle this problem is stated as:

Program 1. Given positive definite polynomials $\varphi_i = \sum_{j=1}^{n} \epsilon_{ij} x_j^{2d}$, for some natural number d and some small real positive coefficients ϵ_{ij}, and a shaping function $s(x)$, a stable closed-loop invariant set $\Omega_\gamma = \{x \in \mathcal{D} | V \leq \gamma\}$ around the origin can be obtained by finding $V \in \Sigma_n$, $K \in \mathbb{R}[x]$ and $q_i \in \Sigma_n$, for $i \in \{1, 2, 3\}$, such that

$$V - \varphi_1 \in \Sigma_n, \tag{2}$$
$$(s - \beta)q_1 - (V - \gamma) \in \Sigma_n, \tag{3}$$
$$-\frac{\partial V}{\partial x}(f + gK)q_2 - \varphi_2 + (V - \gamma)q_3 \in \Sigma_n. \tag{4}$$

The first SOS constraint guarantees positive definiteness of $V(x)$, the second constraint ensures $\{x \in \mathcal{D} | s(x) \leq \beta\} \subset \{x \in \mathcal{D} | V(x) \leq \gamma\}$ and the third restriction enforces negativeness of $\dot{V}$ along with the closed-loop system trajectories. Clearly, one should try to maximize β in order to increase the volume of the RoA.

Constraints (3) and (4) are bilinear in the decision variables due to the products of $\beta\, q_1$, $\nabla_x V\, K\, q_2$ and $(V-\gamma)\, q_3$. The problem can be tractable by decomposing it into sub-steps of convex problems with an iterative bounding procedure. It is an application of block-coordinate descent method (Shen et al. (2017)) that relies on fixing some of the decision polynomials and handle restrictions separately thought an iterative algorithm.

Algorithm 1. **Iterative bounding procedure** (Jarvis-Wloszek et al. (2005)) Choose an initial V_0 candidate and specify the shaping function $s(x)$. Define the degrees of polynomials V, K and q_i. Set φ_i with small coefficients ϵ_i. Proceed to *$\mathcal{K}$-Step*.

- ***$\mathcal{K}$-Step***: Maximize γ with V and q_2 fixed to obtain K such that (4) holds;
- ***γ-Step***: Maximize γ with V and K fixed to obtain γ, q_2 and q_3 such that (4) holds;
- ***β-Step***: Maximize β over q_1 with V and γ fixed to obtain β and q_1 such that (3) holds;
- ***$\mathcal{V}$-Step***: Keep K, γ, β, q_1, q_2, and q_3 fixed and find V such that (2)-(4) hold. If β no longer improves conclude the iterations, otherwise, return to *$\mathcal{K}$-Step*.

2.2 Expanding the RoA with state feedback and input saturation

Expanding the region of attraction with state feedback is a problem that resumes to synthesize a state feedback controller $u = K(x)$ with $K(x) \in \mathbb{R}[x]$ that enlarges the invariant set Ω_γ such that the origin is an asymptotically stable equilibrium point of the closed-loop system.

Recognizing the physical limitations of the vehicle in study, it is necessary to define upper and lower bounds for the control laws. Program 1 must guarantee that $|u_i| \leq u_{i,max}$ where $u_{i,max}$ are the known input bounds and $i \in \{1, ..., m\}$. As shown by Jarvis-Wloszek et al. (2005), taking into account the effect of saturation through the control design procedure, two conditions are obtained:

$$\begin{aligned} \{x \in \mathcal{D} | V(x) \leq \gamma\} \subset \{x \in \mathcal{D} | K_i(x) \leq u_{i,max}\} \\ \{x \in \mathcal{D} | V(x) \leq \gamma\} \subset \{x \in \mathcal{D} | K_i(x) \geq -u_{i,max}\} \end{aligned} \tag{5}$$

These set containment ensures that $|u_i| = |K_i(x)| \leq u_{i,max}$ for all x inside the invariant set $\{x \in \mathcal{D} | V(x) \leq \gamma\}$. In SOS decomposition, the conditions take the form:

$$\begin{aligned} &\big((u_{i,max} - K_i) + (V-\gamma)q_{4,i}\big) \in \Sigma_n, \\ &\big((u_{i,max} + Ki) + (V-\gamma)q_{5,i}\big) \in \Sigma_n, \\ &q_{4,i},\ q_{5,i} \in \Sigma_n. \end{aligned} \tag{6}$$

and must be included in Program 1 when the system is conditioned to input saturation.

3. GROUND VEHICLE MATHEMATICAL MODEL

A ground vehicle may be described by two subsystems. The first describes the body motion by rigid body dynamics and kinematics. The second describes the tire-ground interaction which is the primary source of forces that make the vehicle move.

3.1 Equations of motion

The planar model with lumped axle, also known as bicycle model, is illustrated in Figure 1. It is a simplification of the four-wheel vehicle model and assumes a single tire at each axle with twice the force capability of the individual tires. Rolling and pitching motions are neglected. The bicycle model can be found in many literature works. Some detailed derivations are given in Rajamani (2011) and Liu (2013).

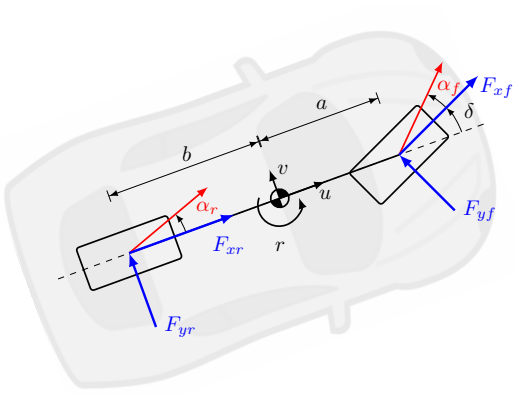

Fig. 1. Diagram of the bicycle model.

The state vector is described in terms of vehicle's longitudinal velocity u, lateral velocity v and yaw rate r which is the rotational velocity around the z-axis, all of them specified at the center of gravity (CG). By inspection, the equations of motion are derived by analyzing balance between forces and moments (Newton-Euler equations) in x, y and z-axis. From Figure 1 we have:

$$\begin{aligned} m(\dot{u} - rv) &= F_{xr} + F_{xf}\cos\delta - F_{yf}\sin\delta, \\ m(\dot{v} + ru) &= F_{yf}\cos\delta + F_{yr} - F_{xf}\sin\delta, \\ I_z\dot{r} &= a(F_{yf}\cos\delta + F_{xf}\sin\delta) - bF_{yr} + cM_z, \end{aligned} \tag{7}$$

where m is the vehicle mass, F_{yi} and F_{xi} are lateral and longitudinal forces and subscripts $i \in \{f, r\}$ denotes front and rear wheels, respectively. I_z is the vehicle's yaw inertia, δ is the front tire steer angle and α_i are the slip angles. Distances a and b are measured from CG to front and rear axles. Constant c is the distance between wheels on the same axle of the equivalent four wheel planar vehicle and M_z is the yaw moment term.

To analyze the vehicle lateral stability, we may linearize the system considering a rectilinear uniform movement (constant longitudinal velocity u_0), resulting in the decoupling of longitudinal and lateral dynamics.

In this work, the stability analysis process focuses on the dynamic characteristics of a electric vehicle with rear independent motorized wheels. As consequence, the front longitudinal force F_{xf} is purely reactive and thus it is acceptable to consider $F_{xf} \approx 0$. Considering the linearization is made for rectilinear uniform motion, the steering angle δ is small. The corresponding lateral dynamics are considerably simplified and described by:

$$\begin{aligned} m(\dot{v} + ru_0) &= F_{yf} + F_{yr}, \\ I_z\dot{r} &= aF_{yf} - bF_{yr} + cM_z. \end{aligned} \tag{8}$$

where the variables now represent variations of the trim condition.

The control inputs are steering angle δ, which indirectly defines the magnitude of F_{yi}, and the yaw moment M_z, achieved by the differential torque.

3.2 Tire forces

The behavior of tire-ground forces interaction has been subject of several studies for their highly nonlinear nature Pacejka (2005); Dugoff et al. (1970); Hirschberg et al. (2007). Typically, they are modeled as a function of their wheel loads, camber and tire slips. This study makes use of the *Magic Formula* (MF) tire model given in Pacejka (2005), an analytical model with well defined characteristics largely applied in academic studies. The MF describes lateral tire forces F_{yi} as a function of the wheel slip angle α_i

$$F_{yi}(\alpha_i) = D\sin(C\arctan(B(1-E)\alpha_i + E\arctan(B\alpha_i))), \tag{9}$$

with $i \in \{f, r\}$ denoting front and rear quantities. Constants B, C, D and E are semi empirical parameters that characterize shape, peak, increasing rate and saturation (see Pacejka (2005)). These parameters follow Ono et al. (1998).

The slip angle (see Figure 1) is characterized by the absolute speed components of the wheel center in a local wheel coordinate system, i.e., it is the angle between the longitudinal u_w and lateral v_w components of the absolute wheel velocity, $\alpha_i = \arctan\frac{v_w}{u_w}$. By considering a planar motion kinematics, the slip angles can be exactly rewritten as:

$$\alpha_f = \arctan\left(\frac{\cos\delta(v + ar) - \sin\delta u}{\cos\delta u + \sin\delta(v + ar)}\right), \tag{10}$$

$$\alpha_r = \arctan\left(\frac{v - br}{u}\right). \tag{11}$$

Given that we are using the linearized lateral dynamics, we may assume small values of α_i, and therefore $\arctan(\alpha_i) \approx \alpha_i$. Expressions (10) and (11) are then simplified to

$$\alpha_f = \frac{v + ar}{u} - \delta, \tag{12}$$

$$\alpha_r = \frac{v - br}{u}. \tag{13}$$

3.3 Polynomial approximation

The SoS theory can only be applied to control affine systems described by polynomial functions. Therefore, (9) must first be approximated by the following function:

$$F_{yi}(\alpha_i) = \sum_{j=0}^{n} p_{ij}\alpha^j = p_{i0} + p_{i1}\alpha_i + p_{i2}\alpha_i^2 + \cdots + p_{in}\alpha_i^q \quad (14)$$

where q is the polynomial order and coefficients p_{ij} can be found with nonlinear least-squares algorithm.

To assemble the complete lateral dynamics model, we need to guarantee that all functions involved are polynomials of their arguments. The ordinary differential equations are obtained by substituting (12) and (13) into polynomial approximation (14) which can then be substituted into (8). The two complete equations achieved describe the lateral dynamics with states $x = [v, r]^T$ and inputs $u = [\delta, M_z]^T$.

It is essential to observe that approximation (14) is a function of states x and input δ, consequently, lateral forces $F_{yi}(x, \delta)$ necessarily contain elements with exponents of order q and terms with arguments $\delta, \delta^2 \dots \delta^q$ will appear. This makes the polynomial model not affine in input δ.

4. INPUT AFFINE APPROXIMATION

The control synthesis problem through SOS decomposition is exclusively intended to affine in control systems, otherwise we fall on a non-convex problem. To keep convexity and the control design a feasible problem we propose an affine approximation.

With the two controls inputs $u_1 = \delta$ and $u_2 = M_z$, the state space representation (1) must be written as

$$\dot{x} = f(x) + g_1(x)u_1 + g_2(x)u_2. \quad (15)$$

By inspection of system (8), input M_z only affects $\dot{r}$, consequently, input vector $g_2(x)$ can be straightforward obtained:

$$\dot{x} = f(x) + g_1(x)\delta + \underbrace{\begin{bmatrix} 0 \\ c/I_z \end{bmatrix}}_{g_2(x)} M_z \quad (16)$$

However, defining $g_1(x)$ requires some abstraction. With the polynomial approximation (14), the control actuation with respect to g_1 will be on the form

$$g_1(x, \delta) = g_{1_1}(x)\delta + g_{1_2}(x)\delta^2 + ... + g_{1_n}(x)\delta^n. \quad (17)$$

To use the tools provided by Algorithm 1, $g_1(x, \delta)$ must be affine in δ. For this reason, (17) is reduced here to its first order approximation near a given steady state $\bar{\delta}$ point

$$g_1(x, \delta) \approx g_1(x, \bar{\delta}) + \left.\frac{\partial g_1}{\partial \delta}\right|_{x,\bar{\delta}} (\delta - \bar{\delta}). \quad (18)$$

Hence, substituting (18) into (16):

$$\dot{x} = \underbrace{f(x) + g_1(x, \bar{\delta}) - \left.\frac{\partial g_1}{\partial \delta}\right|_{x,\bar{\delta}} \bar{\delta}}_{\bar{f}(x)} + \underbrace{\left.\frac{\partial g_1}{\partial \delta}\right|_{x,\bar{\delta}}}_{\bar{g}_1(x)} \delta + g_2(x)M_z, \quad (19)$$

the system may be written as:

$$\dot{x} = \bar{f}(x) + \bar{g}_1(x)\delta + g_2(x)M_z, \quad (20)$$

where $\dot{x}$ is affine in δ and M_z and thus the iterative bounding procedure can be applied. Now we can search for two control laws $K_1(x)$ and $K_2(x)$ that expand the region of attraction of the vehicle system.

5. CONTROL DESIGN APPLICATION

The main rationality about using SOS decomposition is to approximate the RoA by a level set of a Lyapunov function. It is expected that as we choose higher order Lyapunov functions we may improve our representation of the domain of attraction. In a similar form, larger RoAs estimates are expected as we increase the order of the control law $K(x)$. Understanding these characteristics, our results are presented varying the degrees combinations of $V(x)$ and $K(x)$. First we estimate the RoA under an open-loop analysis and further expand it with state feedback and input saturation.

Algorithm 1 requires a candidate shaping function $s(x)$, an initial Lyapunov function $V_0(x)$, polynomials φ_i and the degree specification for polynomials $q_i(x)$.

The shaping function gives dimensional scaling and reflects the influence of certain directions in the state space. Its importance relies on the fact that $s(x)$ provides the shape or mold of the regions over which we will be verifying the Lyapunov conditions. Since it is not intuitive to visualize, we follow the suggestion presented in Masouleh and Limebeer (2017) where a Lyapunov function of lower degree is used as the shaping function when finding higher-order Lyapunov functions, i.e., $s(x)$ is defined as our best second-order $V(x)$, obtained from previous runs, when searching for a $V(x)$ of fourth-order and so on. The idea comes from the fact that as the degree of the Lyapunov function is increased, region $(V(x) - \gamma)$ better aligns with the gradient of our dynamic model and, therefore, is a suitable $s(x)$ candidate for new searches, systematically.

Regarding the choice of $V_0(x)$, following the suggestion made in the majority of works focused on estimating the RoA using SOS constraints, an easy and good choice is the quadratic Lyapunov function $V_{lin} = x^T P x$ derived from the linearized vehicle model associated with the Lyapunov equation (Tamba and Nazaruddin (2018); Iannelli et al. (2019)).

Coefficients ϵ_1 and ϵ_2 are defined as small positive constants around the magnitude of 10^{-6} and the tire force approximation (14) is chosen to be a 7th order polynomial.

In order to satisfy the degree bounds recognized in (2)-(4), the function degrees are defined as:

$$\begin{aligned} \deg(\varphi_1) &= \deg(\mathrm{V}) \\ \deg(q_1) &= \max\{\deg(\mathrm{V}) - \deg(\mathrm{s}), 2\} \\ \deg(q_2) &= 2 \\ \deg(q_3) &= \deg(g_2) + \deg(q_2) + \deg(K_1) - 1 \\ \deg(\varphi_2) &= \deg(q_3) \\ \deg(q_{4,i}) = \deg(q_{5,i}) &= \max\{\deg(V) - \deg(K_1), 2\}, \end{aligned} \quad (21)$$

5.1 RoA estimation

With our configuration now set up, we can evaluate Algorithm 1. The SOS constraints are implemented using SOSTOOLS (Papachristodoulou et al. (2013)) package that

reformulates the problem as a semidefinite programming which is solved via SeDuMi.

The physical vehicle parameters used in this study are listed in Table 1.

Table 1. Vehicle main physical parameters.

Symbol	Parameter name	Value
m	Vehicle mass	1500 kg
I_z	Yaw inertia	3000 $^{kg}/_{m^2}$
a	Distance from CG to front wheels	1.2 m
b	Distance from CG to rear wheels	1.3 m
c	Half of wheelbase distance	0.9 m
δ_{max}	Steering saturation	15 ^{o}
$M_{z_{max}}$	Differential moment saturation	1200 N

As a first application we estimate the RoA of the uncontrolled system ($K(x) = 0$). Steering angle is set to 5 degrees with constant longitudinal speed $u_0 = 10m/s$. For the trim condition selected and using the physical parameters given above, the state matrices of the linearized model are

$$A = \left[\begin{matrix} \frac{\partial f_1}{\partial v} & \frac{\partial f_1}{\partial r} \\ \frac{\partial f_2}{\partial v} & \frac{\partial f_2}{\partial r} \end{matrix}\right]\Bigg|_{(\bar{v},\bar{r})} = \begin{bmatrix} -1.846 & -10.166 \\ -0.0830 & -1.4316 \end{bmatrix}, \quad (22)$$

$$B = \left[\begin{matrix} \frac{\partial g_1}{\partial \delta} & \frac{\partial g_1}{\partial M_z} \\ \frac{\partial g_2}{\partial \delta} & \frac{\partial g_2}{\partial M_z} \end{matrix}\right]\Bigg|_{(\bar{\delta},\bar{M}_z)} = \begin{bmatrix} 10.263 & 0 \\ 6.158 & 0.25 \times 10^{-3} \end{bmatrix}, \quad (23)$$

given with the international system units.

Figure 2 shows the RoA estimates. The phase portrait of the polynomial vehicle model is shown in background along with the equilibrium points denoted by black dots.

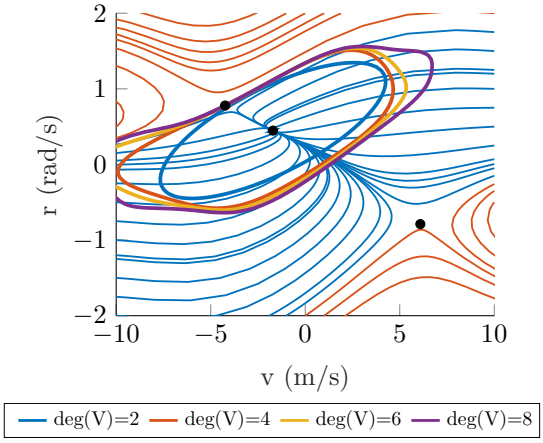

Fig. 2. RoA estimates for a cornering maneuver. Steering angle is set at 5 degrees, longitudinal speed $u_0 = 10m/s$. Shaping function $s(x)$ is chosen to be the Lyapunov function of lower degree.

It can be noted that the RoA estimates become more representative as we increase the degree of $V(x)$. When we choose $s(x)$ to be the best $V(x)$ of lower order, restriction (3) ensures that the new Lyapunov function with higher degree will contain the previous one. To quantify these improvements, we propose comparing surfaces area of the estimated RoA. Table 2 shows the improvement we obtain as advancing in the search of $V(x)$ of higher orders.

Table 2. Rising area of the estimated RoA as increasing the order of polynomial $V(x)$.

deg(V)	2	4	6	8
Area	11.6949	16.3942	18.6345	21.0372

By increasing the order of $V(x)$, the number of decision variables of the resulting SDP grows rapidly. The combination of this characteristic with the fact that system (1) was assembled as a seventh-order polynomial vector field turns our restrictions strongly sensitive to a relative change in x and, as consequence, numerical scaling failure is more likely to occur. Unfortunately, computational growth is still a generic trend in SOS optimizations.

5.2 Expanding the RoA with state feedback

We will now focus our attention on expanding the RoA with state feedback and input saturation. In an attempt to get better estimates, as discussed above, $s(x)$ is bootstrapped by the previous Lyapunov function. Again, steering angle is set to +5 degrees with constant longitudinal velocity $u = 10m/s$. The controller saturation limits are $|u_{1,max}| \leq 15$ degrees and $|u_{2,max}| \leq 1200N$.

Figure 3 shows the RoA estimates for certain degrees of K_i and V. It is straightforward to verify that RoA estimates are indeed increased with a state feedback controller.

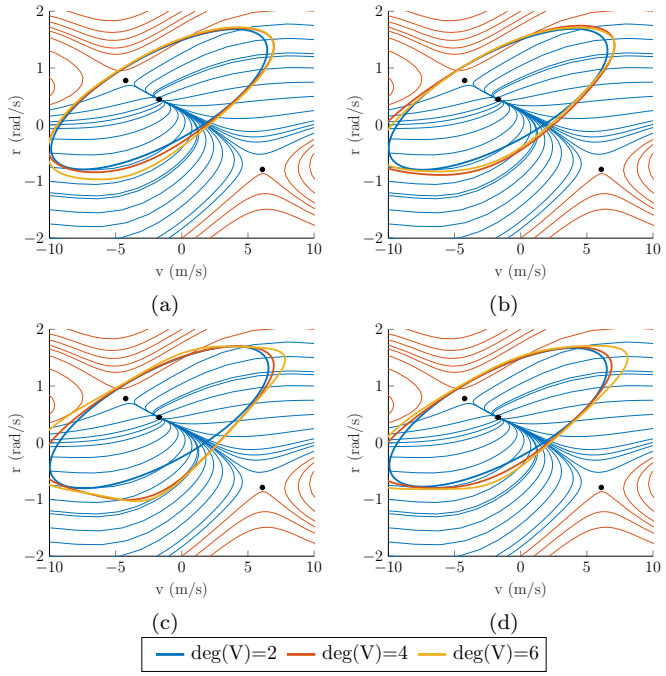

Fig. 3. Estimated stability regions of the controlled system. Lyapunov functions are shown for different degrees. RoA is estimated by considering a control laws K_i of (a) degree 1, (b) degree 2, (c) degree 3 and (d) degree 4.

Increasing the controller degree slightly expand the RoA estimates. In fact, higher order polynomial controller contains the lower ones, thus RoA is indeed expected to increase as far as numerical ill-conditioning arises. For these simulations, searching for a Lyapunov function of order 8 resulted in numerical failure. The rational for this failure

is that, by growing the order of K and V, high degree monomials are used in the SOS program, as consequence, the number of variables increases and the order of the polynomial coefficients become vastly different.

Table 3 shows the area of the RoA estimates as a metric of comparison. It follows that the area increases as we increase the order of polynomials $K_i(x)$ and $V(x)$. As expected, increasing the Lyapunov function order gives a more representative estimative of the RoA and, similarly, increasing the $K_i(x)$ order also potentially leads to improvement since we widen the search space. According to Table 3 this is partially true. For $K_i(x)$ and $V(x)$ of order 4 and 6, respectively, the algorithm ran into numerical problems (by the same reasons discussed above) and the estimation is compromised, noticed by the decrease in RoA estimation.

Table 3. Area of the estimated RoA under a polynomial state feedback controller of arbitrary degree.

		deg(V)		
		2	**4**	**6**
deg(K)	**1**	22.5626	24.2682	26.0119
	2	23.2137	27.4919	25.7333
	3	23.3177	27.8489	30.2255
	4	22.7976	25.0768	27.7607

In practice, the preferred controller would be chosen according to its ability to expand the region of attraction. Clearly, the larger the RoA's area, the larger the set of initial conditions for which the controller will asymptotically stabilize the system. Additionally, one concern in control system design is the numerical conditioning of the control gains. The numerical results are shown in Table 4 and occasional ill-conditioning of the gain matrix has not been observed.

Table 4. Polynomial controller gains K_i of degrees varying from 1 to 4 obtained with the sixth-order Lyapunov Functios.

K_i of degree 1
$K_1(x) = -0.038v + 0.099r$
$K_2(x) = 154.39v - 839.35r$
K_i of degree 2
$K_1(x) = 1.69 \times 10^{-3}v^2 - 0.04vr + 0.06r^2 - 0.01v + 0.03r$
$K_2(x) = -5.24v^2 + 84.43vr - 172.28r^2 + 101.14v - 814.33r$
K_i of degree 3
$K_1(x) = 0.006v^2r - 0.03vr^2 + 0.07r^3 - 0.04vr + 0.07r^2 - 0.003v - 0.04r$
$K_2(x) = -1.39v^3 + 2.09v^2r + 36.29vr^2 - 75.80r^3 - 4.55v^2 + 70.89vr -$ $-218.28r^2 + 134.05v - 637.57r$
K_i of degree 4
$K_1(x) = -2 \times 10^{-4}v^4 + 2.6 \times 10^{-4}v^3r + 0.01v^2r^2 - 0.05vr^3 + 0.07r^4 - 1.9 \times 10^{-4}v^3 +$ $+0.01v^2r - 0.06vr^2 + 0.13r^3 + 3.1 \times 10^{-3}v^2 - 0.02vr - 0.02r^2 - 0.01v + 0.11r$
$K_2(x) = 0.1v^4 - 0.96v^3r - 6.5v^2r^2 + 73vr^3 - 111.4r^4 - 0.25v^3 - 6.54v^2r +$ $+73.59vr^2 - 220.30r^3 - 7.94v^2 + 87.12vr - 184.51r^2 + 82.47v - 395.69r$

The control gains magnitude is explained by its corresponding inputs. $K_1(x)$ is with respect to input δ, expressed in radians, and $K_2(x)$ with respect to M_z with maximum value of $1.2k$N.

6. SOS VS LQR CONTROL PERFORMANCE

We now wish to compare the control synthesis using SOS decomposition with other known control design technique. Among the optimal controllers in control theory, the linear quadratic regulator (LQR) is a well-known design approach that provides practical feedback gains. The controller is designed for a linear model of the system, described by matrices (22) and (23).

Control gain is calculated by $K = R^{-1}B^TP$ where P can be found by solving the continuous time algebraic Riccati equation. The quadratic components, Q and R, that establish a compromise between control effort and performance, are chosen to be:

$$Q = \begin{bmatrix} 5 & 0 \\ 0 & 50 \end{bmatrix}, \; R = \begin{bmatrix} 1 \times 10^3 & 0 \\ 0 & 4 \times 10^{-3} \end{bmatrix}, \tag{24}$$

which allow K to be straightforwardly computed. Q and R are with the international system units.

Given the control gain, the iterative procedure reduces the complexity considerably. With K_1 and K_2 fixed, the controller synthesis step ($\mathcal{K}$-*Step*) is summarized to find polynomials $q_{4,i}$ and $q_{5,i}$, such that (4) and (6) hold. The number of decision variables is now constant. The remaining steps of Algorithm 1 follow normally.

Figure 4 shows the estimated RoA under an LQR closed-loop controller. Comparing to Figure 3, the region is very similar in shape and alignment, but not in size. The estimated RoA clearly comprehends the upper saddle point and surpasses the boundary of the uncontrolled plant, however, due to the fixed controller law, the algorithm quickly converges.

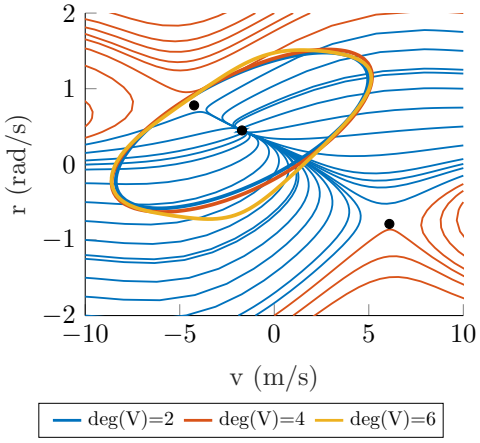

Fig. 4. Estimated stability region of the system with an LQR feedback controller. Lyapunov functions are shown for different degrees.

The areas of the estimated RoAs are shown in Table 5. As expected, the region enlarges as we increase the Lyapunov function order. Comparing with the areas of Table 3, the estimated RoA under an LQR control gain is remarkably lower. The reason is simple: Algorithm 1 works by expanding the domain of attraction Ω_γ and then finding the largest level set of the resulting Lyapunov function that is contained in Ω_γ. Evidently, the estimated region under the SOS closed-loop analysis should be more representative when comparing to LQR, which is not designed for this purpose.

Table 5. Rising area of the estimated RoA as increasing the order of polynomial $V(x)$ under an LQR closed-loop gain.

deg(V)	2	4	6
Area	16.3337	17.6150	18.7786

7. CONCLUSION

In this work, we have shown how the sum of squares technique can be used to analyze the stability of a nonlinear vehicle system.

The methodology, based on the construction of appropriate Lyapunov function certificates, is carried out using sum of squares techniques through SOSTOOLS package. Furthermore, estimating the region of attraction and designing a state feedback control law were explored algorithmically.

The ordinary differential equations of the well-known bicycle dynamic model are presented and the system is approximated to a polynomial vector field. The mathematical system falls on a class of nonaffine-in-input system and control design using SOS decomposition cannot be handled directly. We then propose an affine linearization and the numerical issues and ill-conditioning coming from this solution are discussed. Moreover, the proposed controller design includes the nonlinearities comprised by input constraints associated with the system actuator dynamics.

The work done so far has presented algorithmic solutions to stability analysis and control synthesis for a vehicle model. Future work will be focused on the class of rational polynomial systems and how it can be structured so that the resulting semidefinite programming conditions are numerically well-conditioned.

REFERENCES

Ahmadi, A.A. and Majumdar, A. (2019). DSOS and SDSOS optimization: More tractable alternatives to sum of squares and semidefinite optimization. *SIAM Journal on Applied Algebra and Geometry*, 3(2), 193–230.

Dugoff, H., Fancher, P., and Segel, L. (1970). An analysis of tire traction properties and their influence on vehicle system dynamics. *SAE-paper700377*.

Hirschberg, W., Rill, G., and Weinfurter, H. (2007). Tire model TMeasy. *Vehicle System Dynamics*, 45, 101–119.

Iannelli, A., Marcos, A., and Lowenberg, M. (2019). Robust estimations of the region of attraction using invariant sets. *Journal of the Franklin Institute*, 356(8), 4622–4647.

Jarvis-Wloszek, Z., Feeley, R., Tan, W., Sun, K., and Packard, A. (2005). Control applications of sum of squares programming. In *Positive Polynomials in Control*, 3–22. Springer.

Johnson, D.B. and Huston, J.C. (1984). Nonlinear lateral stability analysis of road vehicles usingb liapunov's second method. In *SAE Technical Paper Series*. SAE International.

Jones, M. and Peet, M.M. (2019). Using sos and sublevel set volume minimization for estimation of forward reachable sets. *IFAC-PapersOnLine*, 52(16), 484 – 489. 11th IFAC Symposium on Nonlinear Control Systems.

Khalil, H.K. (2002). *Nonlinear systems*, volume 3. Prentice hall Upper Saddle River, NJ.

Khodadadi, L., Samadi, B., and Khaloozadeh, H. (2014). Estimation of region of attraction for polynomial nonlinear systems: A numerical method. *ISA Transactions*, 53(1), 25–32.

Landry, B., Chen, M., Hemley, S., and Pavone, M. (2018). Reach-avoid problems via sum-or-squares optimization and dynamic programming. In *2018 IEEE/RSJ International Conference on Intelligent Robots and Systems (IROS)*. IEEE.

Liu, W. (2013). *Introduction to hybrid vehicle system modeling and control*. John Wiley & Sons.

Masouleh, M.I. and Limebeer, D.J.N. (2017). Region of attraction analysis for nonlinear vehicle lateral dynamics using sum-of-squares programming. *Vehicle System Dynamics*, 56(7), 1118–1138.

Németh, B., Gáspár, P., and Péni, T. (2016). Nonlinear analysis of vehicle control actuations based on controlled invariant sets. *International Journal of Applied Mathematics and Computer Science*, 26(1), 31–43.

Nikravesh, S.K.Y. (2018). *Nonlinear Systems Stability Analysis*. CRC Press.

Ono, E., Hosoe, S., Tuan, H.D., and Doi, S. (1998). Bifurcation in vehicle dynamics and robust front wheel steering control. *IEEE transactions on control systems technology*, 6(3), 412–420.

Pacejka, H. (2005). *Tire and vehicle dynamics*. Elsevier.

Papachristodoulou, A. (2005). *Scalable analysis of nonlinear systems using convex optimization*. Ph.D. thesis, California Institute of Technology.

Papachristodoulou, A., Anderson, J., Valmorbida, G., Prajna, S., Seiler, P., and Parrilo, P. (2013). *SOSTOOLS: Sum of squares optimization toolbox for MATLAB*.

Parrilo, P.A. (2003). Semidefinite programming relaxations for semialgebraic problems. *Mathematical Programming*, 96(2), 293–320.

Rajamani, R. (2011). *Vehicle dynamics and control*. Springer Science & Business Media.

Sadri, S. and Wu, C.Q. (2012). Lateral stability analysis of on-road vehicles using lyapunov's direct method. In *2012 IEEE Intelligent Vehicles Symposium*, 821–826. IEEE.

Shen, X., Diamond, S., Udell, M., Gu, Y., and Boyd, S. (2017). Disciplined multi-convex programming. In *2017 29th Chinese Control And Decision Conference (CCDC)*. IEEE.

Singh, S., Chen, M., Herbert, S., Tomlin, C., and Pavone, M. (2019). Robust tracking with model mismatch for fast and safe planning: an sos optimization approach.

Summers, M.E. (2013). *Performance Analysis of Nonlinear Systems Combining Integral Quadratic Constraints and Sum-of-Squares Techniques*. Ph.D. thesis, EECS Department, University of California, Berkeley.

Tacchi, M., Marinescu, B., Anghel, M., Kundu, S., Benahmed, S., and Cardozo, C. (2018). Power system transient stability analysis using sum of squares programming. In *2018 Power Systems Computation Conference (PSCC)*. IEEE.

Tamba, T.A. and Nazaruddin, Y.Y. (2018). Nonlinear stability analysis of vehicle side-slip dynamics using SOS programming. In *2018 5th International Conference on Electric Vehicular Technology (ICEVT)*. IEEE.